Available online at www.sciencedirect.com
SCIENCE DIRECT®
International Journal of Thermal Sciences 44 (2005) 477–490
International Journal of Thermal Sciences
www.elsevier.com/locate/ijts

# Mechanical smoke exhaust for small retail shop fires

C.L. Shi [a], Y.Z. Li [a], R. Huo [a], B. Yao [a], W.K. Chow [b,*], N.K. Fong [b]

[a] *State Key Laboratory of Fire Science, University of Science and Technology of China, Hefei 230026, China*
[b] *Department of Building Services Engineering, The Hong Kong Polytechnic University, Hong Kong, China*

Received 14 July 2003; received in revised form 12 October 2004; accepted 12 October 2004

**Abstract**

The operation of mechanical exhaust in a small retail shop fire will be studied with a two-layer model. Different equations on axisymmetric fire plume entrainment and spill plume will be considered. A zone model has been developed to predict the fire growth in retail shops. Correlation between the mechanical exhaust rate and plume entrainment rate for keeping the smoke layer interface at a certain height under a steady burning fire will be analyzed.

A series of full-scale burning tests were carried out in a chamber with a vertical vent. In addition to validating the developed model, the results will also be compared with those predicted by another zone model CFAST. The effectiveness of mechanical exhaust in retail shop fires will be discussed. How different plume correlations can be applied will be investigated and compared. Some factors affecting the calculation will also be analyzed.


*Keywords:* Mechanical exhaust; Plume correlation; Smoke outflow; Steady height

## 1. Introduction

Many retail shops are constructed at the floor level in big malls where there are difficulties in designing smoke extraction systems for the entire space. An accidental fire in a shop might have smoke spreading out of the shop to other parts of the mall. Mechanical smoke exhaust is necessary for retail shops in those malls. Proper design might give a high enough clear height by operating the mechanical extraction system, which becomes the design objective. It is interesting to see how this design objective can be achieved for retail shops in big malls, especially in places like China or Hong Kong where there are so many such malls and performance-based fire safety design can be applied. For assessing the design, the correlation of smoke production rate and mechanical exhaust rate would be helpful to understand the development of smoke layer.

The smoke production rate can be calculated by various plume models such as Zukoski's correlation [1], Heskestad's correlation [2], McCaffrey's correlation [3] and Thomas's correlation [4], which were used in many fire zone models. For example, for the two-layer zone model CFAST [5], McCaffrey's correlation for calculating the plume entrainment rate was used. Among these plume correlations, some are derived from theoretical analytical studies, while some are empirical formulas based on experiments, so different entrainment rates will be predicted even for the same fire. This will have deviation in predicting for the smoke filling and smoke control, which will give rise to uncertainty for building fire safety design. Also, the real fire environments in a retail shop with mechanical exhaust are always different from the free space. Interaction of the mechanical exhaust and the air flow through door opening would give different flow rates of smoke in comparison with the predictions.

In this paper, full-scale fire experiments are performed to investigate the effects of mechanical exhaust in a well-ventilated retail shop built in the PolyU/USTC Atrium, a joint collaboration project between University of Science

* Corresponding author.
*E-mail address:* bewkchow@polyu.edu.hk (W.K. Chow).

1290-0729/$ – see front matter 
doi:10.1016/j.ijthermalsci.2004.10.002

**Nomenclature**

| | | |
|---|---|---|
| $A_c$ | area of ceiling | $m^2$ |
| $A_e$ | area of mechanical vent | $m^2$ |
| $A_s$ | surface area of upper layer | $m^2$ |
| $b$ | half width of plume | |
| $C$ | coefficient in Eq. (41) | |
| $C_d$ | effective coefficient of discharge in Eq. (17) | |
| $C_e$ | constant in Eq. (15) | |
| $C_f$ | constant in Eq. (7) | |
| $C_i$ | correction coefficient for $M_p$ due to $M_i$ when interface fluctuates greatly | |
| $C_p$ | specific heat capacity | $kJ\cdot kg^{-1}\cdot K^{-1}$ |
| $D_f$ | diameter of fire | m |
| $g$ | acceleration due to gravity | $m\cdot s^{-2}$ |
| $h$ | height | m |
| $H_c$ | height of ceiling | m |
| $H_e$ | height of mechanical vent | m |
| $H_{em}$ | middle height of mechanical vent to ground | m |
| $H_k$ | effective coefficient of convective heat transfer | $kW\cdot m^{-2}\cdot K^{-1}$ |
| $H_s$ | depth of spill plume | m |
| $H_v$ | height of ventilation opening | m |
| $H_n$ | height of neutral profile | m |
| $L$ | distance from radiometer to fire source center | m |
| $m$ | mass of upper layer | kg |
| $\dot{M}_e$ | mechanical exhaust rate | $kg\cdot s^{-1}$ |
| $\dot{M}_i$ | mass exchange rate at the interface | $kg\cdot s^{-1}$ |
| $\dot{M}_f$ | mass flow rate induced by fire burning | $kg\cdot s^{-1}$ |
| $\dot{M}_p$ | mass flow rate of plume into upper layer | $kg\cdot s^{-1}$ |
| $\dot{M}_s$ | mass flow rate of spill plume | $kg\cdot s^{-1}$ |
| $\dot{m}_f$ | transient mass loss rate of fire source | $kg\cdot s^{-1}$ |
| $P_f$ | perimeter of fire source | m |
| $P_e$ | perimeter of enclosure | m |
| $\dot{Q}$ | total heat release rate | kW |
| $\dot{Q}_c$ | convective heat release rate | kW |
| $\dot{Q}_{\text{Loss}}$ | heat loss rate | kW |
| $\dot{q}_r$ | radiation measured by radiometer | $kW\cdot m^{-2}$ |
| $T_s$ | temperature of hot smoke layer | K |
| $T_0$ | ambient air temperature | K |
| $V_e$ | velocity of mechanical vent | $m\cdot s^{-1}$ |
| $V_s$ | horizontal velocity of spill plume | $m\cdot s^{-1}$ |
| $W$ | width of ventilation opening | m |
| $w$ | upward velocity of plume | $m\cdot s^{-1}$ |
| $Z$ | height of smoke layer interface | m |
| $Z'$ | calculated distance from fire to smoke layer interface | m |
| $Z_b$ | elevation of fire bottom to ground | m |
| $Z_0$ | elevation of virtual origin location | m |
| $Z_{0,f}$ | virtual origin for near field plume of Zukoski | m |
| $Z_{fl}$ | effective flame height | m |

*Greek letters*

| | | |
|---|---|---|
| $\alpha$ | combustion efficiency | |
| $\lambda_c$ | coefficient for convective heat release rate | |
| $\lambda_r$ | coefficient for radiative heat release rate | |
| $\rho_s$ | density of hot smoke layer | $kg\cdot m^{-3}$ |
| $\rho_0$ | density of ambient air | $kg\cdot m^{-3}$ |
| $\Delta H_c$ | heat of combustion | $kJ\cdot kg^{-1}$ |
| $\Delta T$ | excess temperature of plume | K |
| $\Delta\rho$ | density deficit of plume | $kg\cdot m^{-3}$ |
| $\phi$ | expression of plume models in Eq. (32) | |
| $\gamma, \eta$ | exponent in Eq. (41) | |

and Technology of China (USTC) and The Hong Kong Polytechnic University (PolyU). With different plume entrainment correlations along with spill plume correlation, a zone model has been developed to investigate the fire environment. Through studying the result of experiments and calculations, the effectiveness of mechanical exhaust in shop fires is discussed, and the applicability of different plume correlations is compared. Some factors affecting the calculation are also analyzed.

## 2. Simplified model of mechanical exhaust

The two-layer model [6,7] developed previously is used to analyze the smoke control by mechanical exhaust in a shop under fire. Basic phenomena and terminology are illustrated in Fig. 1. There are basically two layers: the upper hot smoke layer and the lower air layer. Thermal-stratification phenomenon was well observed by salt water modeling [8].

Mass conservation equation for the upper hot smoke layer is:

$$\frac{\mathrm{d}m}{\mathrm{d}t} = \begin{cases} \dot{M}_p + \dot{M}_i \\ \quad (H_{em} + H_e/2 < Z < H_c) \\ \dot{M}_p + \dot{M}_i - \left[(H_{em} + H_e/2 - Z)/H_e\right]\dot{M}_e \\ \quad (H_{em} - H_e/2 < Z < H_{em} + H_e/2) \\ \dot{M}_p + \dot{M}_i - \dot{M}_e \\ \quad (H_v < Z < H_{em} - H_e/2) \\ \dot{M}_p + \dot{M}_i - \dot{M}_e - \dot{M}_s \\ \quad (Z_0 + Z_b < Z < H_v) \end{cases} \tag{1}$$

The smoke production rate from the fire source, $\dot{M}_f$, is very small in comparison with the entrainment rate to the plume, which can be neglected in most cases.

Energy conservation in the upper layer gives:

$$mC_p\frac{\mathrm{d}T_s}{\mathrm{d}t} = \dot{Q}_c - \left(\dot{M}_p + \dot{M}_i\right)C_p(T_s - T_0) - H_k A_s(T_s - T_0) \tag{2}$$

Assuming the heat lost of the smoke layer by radiation, convection and conduction are uniform, $H_k$ is the overall effective heat transfer coefficient averaged on the surfaces with

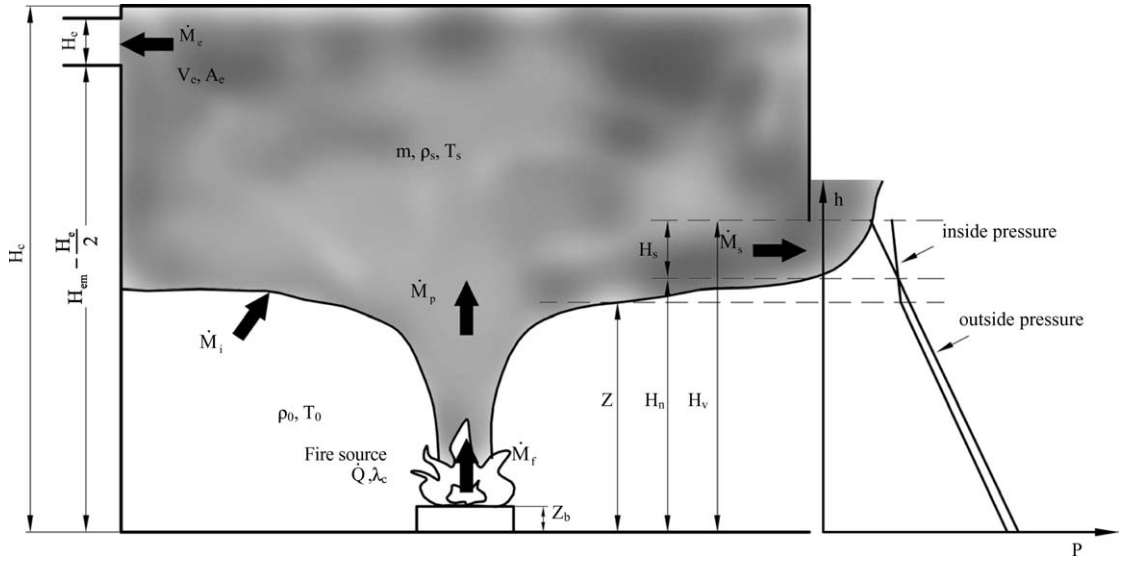


Fig. 1. The two-layer zone model.

area $A_s$, the surface area of the upper layer. $H_k$ is related to the surface material and the Rayleigh number and assumed to be a constant.

When the mass inflow rate of the smoke layer is equal to the mass outflow rate, the upper layer interface will be kept at a certain elevation $Z$, the mass balance becomes:

$$\dot{M}_p + \dot{M}_i = \dot{M}_e + \dot{M}_s \tag{3}$$

Heat balance in the steady burning stage of pool fires may be expressed as:

$$\dot{Q}_c = \left(\dot{M}_p + \dot{M}_i\right) C_p (T_s - T_0) + H_k A_s (T_s - T_0) \tag{4}$$

If the disturbance of mechanical exhaust and ventilation opening to the smoke layer is not too strong, $\dot{M}_i$ may also be neglected.

The mechanical exhaust rate $\dot{M}_e$ can be calculated from the extraction velocity $V_e$ and the area of mechanical vent:

$$\dot{M}_e = \rho_s \times V_e \times A_e \tag{5}$$

For fire sources not placed next to the wall, the plume did not tilt too much due to the induced air inflow pattern. The plume mass entrainment rate $\dot{M}_p$ can be calculated using the unbounded free plume correlations, which are usually expressed as a function of the smoke layer height $Z$ and the heat release rate $\dot{Q}$ or the fire diameter $D_f$. In this paper, four typical plume models will be introduced into the conservation equation to predict the development of the upper layer temperature and interface height in the retail shop. The effectiveness of smoke control by mechanical exhaust will then be analyzed theoretically. The four plume models are reviewed to give a better understanding of the theories and application limits.

### 2.1. Zukoski's correlation

Based on the weak plume theory suggested by Morton et al. [9], the buoyant plume of far field was assumed by Zukoski et al. [1] to have a similarity between excess temperature $\Delta T$ and upward velocity $w$. Gaussian Profiles can be fitted in the radial direction with half width, $b$. Entrainment rates were measured by an exhaust hood for diffusional flames of methane stabilized on porous-bed burners of 0.10 to 0.50 m diameter, heat release rates varied from 10 to 200 kW. The mass flow rates were measured for a range of elevations starting just below the top of flame and extending to six times the flame height. Based on their experimental results, a correlation was developed for axisymmetric plumes for far field:

$$\dot{M}_p = 0.076 \dot{Q}^{1/3} (Z - Z_0)^{5/3} \tag{6}$$

The location of the virtual origin $Z_0$ was suggested by Cetegen et al. [10] as:

$$\begin{aligned} \dot{Q}/D_f^{2/5} &\geqslant 1105, \qquad Z_0 = 0.066 \dot{Q}^{2/5} - C_f D_f \\ \dot{Q}/D_f^{2/5} &< 1105, \qquad Z_0 = 0.01\left(\dot{Q}/D_f\right)^{2/3} - C_f D_f \end{aligned} \tag{7}$$

For fires at the floor, $C_f = 0.50$; and for fires above the floor, $C_f = 0.80$.

To obtain a correlation for fire plume, experimental data were reviewed by Cetegen et al. [10]. Experimental data were correlated by an equation of the form developed by Thomas [4], but rewritten with the origin for fire plume:

$$\dot{M}_p = 0.62 D_f (Z - Z_{0,f})^{3/2} \tag{8}$$

However, the data were not sufficient to give accurate $Z_{0,f}$. The following correlation with no $Z_{0,f}$ was proposed for the fire plume region based on their experiments:

$$\dot{M}_p = 0.62 D_f Z^{3/4} \tag{9}$$

The curves of Eqs. (6) and (9) would logically cross at the position near the top of the flame.

### 2.2. Heskestad's correlation

Buoyancy, continuity, momentum and energy conservation equations were reviewed by Heskestad [2] for the fire plume. Agreement could be improved if the analysis was based on the similarity between upward velocity $w$ and density difference $\Delta\rho$, instead of the similarity between excess temperature $\Delta T$ and upward velocity $w$. The Boussinesq approximation for weak point plume was removed so that large density differences can be taken into account. This meant that $\rho_0 = \rho$ was not assumed in some equations. The equations discussed were can be used to describe strong plumes. A correlation was developed for entrainment in fire plume with virtual origin based on large-scale experiments involving relatively high heat release rates and realistic fuel packages:

$$\dot{M}_p = 0.071\dot{Q}_c^{1/3}(Z - Z_0)^{5/3} + 0.0018\dot{Q}_c \tag{10}$$

$$Z_0 = 0.083\dot{Q}^{2/5} - 1.02D_f \tag{11}$$

The mass flow rate depends on the convective heat release rate $\dot{Q}_c$ instead of the total heat release rate $\dot{Q}$ as radiation loss would play a role in real fires. The coefficient $\lambda_c$ for convective heat release rate was confirmed to be about 0.7 by experiments in this paper.

For the reacting, flaming region where the elevations are lower than the effective flame height $Z_{fl}$, Heskestad's correlation gives:

$$\dot{M}_p = 0.0054\dot{Q}_c Z/Z_{fl} \tag{12}$$

$$Z_{fl} = -1.02D_f + 0.235\dot{Q}^{2/5} \tag{13}$$

Heskestad's correlation was listed in NFPA 92B [6].

### 2.3. McCaffrey's correlation

Experimental data were used by McCaffrey (1983) [3] with dimensional analysis to arrive at plume relationships for upward velocity and temperature. Local values of velocity and density at different elevations and radial positions in the adiabatic plume and fire plume were measured directly, and then used to obtain time-averaged estimates of density $\bar{\rho}\{r, Z\}$ and velocity $\overline{w}\{r, Z\}$ profiles. Integrating the product over the area of the plume gave an estimation of the total mass flux in the plume.

By dimensional analysis, the plume was divided into three regions: the continuous flame region, the intermittent region, and the plume. The coefficients were obtained by fitting of the experimental data. Methane flames of heat release rates 14.4, 21.7, 33.0, 44.9 and 57.5 kW were used in his experiment. The correlations of plume of different regions were of the form:

Continuous flame region:

$$\dot{M}_p/\dot{Q} = 0.011\left(Z/\dot{Q}^{2/5}\right)^{0.566}, \qquad 0 \leqslant Z/\dot{Q}^{2/5} < 0.08$$

Intermittent flame region:

$$\dot{M}_p/\dot{Q} = 0.026\left(Z/\dot{Q}^{2/5}\right)^{0.909}, \qquad 0.08 \leqslant Z/\dot{Q}^{2/5} < 0.20$$

Smoke plume region:

$$\dot{M}_p/\dot{Q} = 0.124\left(Z/\dot{Q}^{2/5}\right)^{1.895}, \qquad 0.20 \leqslant Z/\dot{Q}^{2/5} \tag{14}$$

It should be noted that in McCaffrey's plume equations, the plume properties are assumed to be independent of fuel, and only dependent on energy release rate, $\dot{Q}$. Since flames from different fuels have different luminosity, radiation losses vary considerably between fuels. Therefore, flame temperature varies from fuel to fuel. Fuel effects were not marked in regions above the continuous flame region.

### 2.4. Thomas's correlation

Experimental data used to derive the above plume equations did not include conditions where the mean flame height, $Z_{fl}$, was significantly less than the fuel source diameter. In the continuous flame region, or in the near field, the plume mass flow rate was found by Thomas et al. [4] to be independent of the energy release rate, but more as a function of the perimeter of the fire, $P_f$, and the height above the fire source, $Z$. This had been found to be very obvious for fires where the mean flame height is considerably smaller than the diameter. The plume mass flow rate equation by Thomas was written as:

$$\dot{M}_p = 0.188Z^{3/2}P_f \tag{15}$$

Note that the plume shape was no longer assumed to be conical, but cylindrical. This is typical for larger fires, where the flame height tends to be lower than the fire diameter.

It is observed that the mass flow rates predicted by Thomas were only valid up to the flame tip. The predicted mass flow rates above this height had also been found to agree well with the data. For example, $Z$ was up to $10\sqrt{A_f}$ for fires in large space in heat release rate 110–750 kW. The entrainment correlation might be extended as the following:

$$\dot{M}_p = C_e Z^{3/2}P_f \tag{16}$$

The coefficient $C_e$ is 0.188 for large spaces such as auditoria, stadia, large open-plan offices and atria, where the ceiling is well above the fire. $C_e = 0.210$ for large-space rooms, such as open-plan offices, where the ceiling is close to the fire. $C_e = 0.337$ for small-space rooms such as unit shops, cellular offices and hotel bedrooms with ventilation openings predominantly to one side of the fire; which is the value used in this paper.

The equation is relatively simple and useful for cases where $Z_{fl}/D_f < 1$ and for cases where the fire source is noncircular.

### 2.5. Vertical vent outflow

When the hot layer descends to the elevation of door opening, the hot smoke will be driven to flow out by the pressure difference across the vent. By Bernoulli's equation,

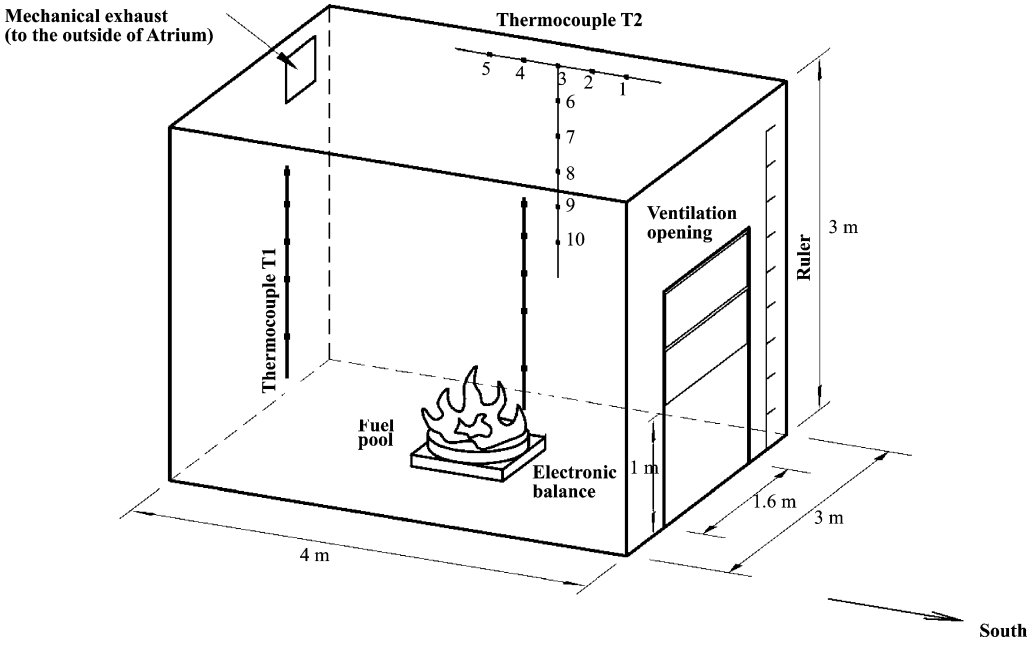


Fig. 2. Schematic diagram of the experiment setup.

the outflow velocity $V(h)$ at the elevation h to the neutral plane is:

$$V(h) = C_d\sqrt{\left[2h(\rho_0 - \rho_s)g\right]/\rho_s} = C_d\sqrt{2hg(T_s/T_0 - 1)} \quad (17)$$

Then, the average outflow velocity $V_s$ can be obtained by the integral of $h$ from the neutral plane to the soffit of vent:

$$V_s = \frac{2}{3}C_d\sqrt{2H_s g(T_s/T_0 - 1)} \quad (18)$$

Approximately, the position of the neutral plane is considered as the soffit of the spill plume at the vent section, that is:

$$H_n = H_v - H_s \quad (19)$$

So, the mass flow rate of spill plume $\dot{M}_s$ may be derived from the average spill velocity.

$$\dot{M}_s = \rho_s V_s H_s W = \frac{2}{3}C_d\rho_s H_s^{3/2} W\sqrt{2g(T_s/T_0 - 1)} \quad (20)$$

where $C_d$ [11] is the effective coefficient of discharge for the vertical opening. In this paper, by the measurement of the horizontal average outflow velocity in previous experiments, $C_d$ was taken as 0.7.

## 3. Experimental setup

Experiments are performed in a shop model of length 4 m, width 3 m and height 3 m as illustrated in Fig. 2. The model is made of steel. The roof and the walls are made of double-deck fireproof gypsum boards of 7 cm thick, with an air void of 5 cm thick. This model was jointly built by University of Science and Technology of China and The Hong Kong Polytechnic University for investigating retail shop fires.

As shown in Fig. 2, two racks of thermocouples labeled as T1 and T2 were mounted on the shop wall to measure the temperature distributions. T1 was mounted on the west wall with 10 T-type thermocouples of 1.5 mm diameter arranged as two vertical sets and distributed at intervals of 5, 40, 40, 40 and 60 cm from the shop roof. The two sets trisected the west wall horizontally. T2 also had 10 T-type thermocouples of 1 mm diameter mounted on the east wall and arranged in a T-shape. The top five thermocouples labeled as 1 to 5 were put at 40 cm horizontal intervals from each other, and 5 cm down the ceiling from south to north. The middle five thermocouples labeled as 6 to 10 were arranged with vertical intervals of 35, 40, 40, 40 and 60 cm.

It is difficult to install an exhaust hood in the atrium to measure the heat release rate by the oxygen consumption method. The transient mass loss rate of fuel was measured by an electronic balance during the burning process to calculate the total heat release rate. The uncertainty of measuring the heat release rate by the mass heat lost rate method is about 5%. This value was confirmed by measuring the heat release rate for a 0.3 m by 0.3 m pool diesel fire by the oxygen consumption method with a room calorimeter. The 0.6 m by 0.6 m diesel pool fire would have a combustion efficiency $\alpha$ of 90%. But for smaller pool fires, the values of $\alpha$ would increase. For burning diesel as in this set of experiments, sufficient air was supplied through the door for combustion. The flame was found to give not so many smoke particulates than from big diesel pool fires of sizes up to 0.6 m by 0.6 m. The combustion efficiency $\alpha$ can be approximated as the value of 1, having 5% uncertainty.

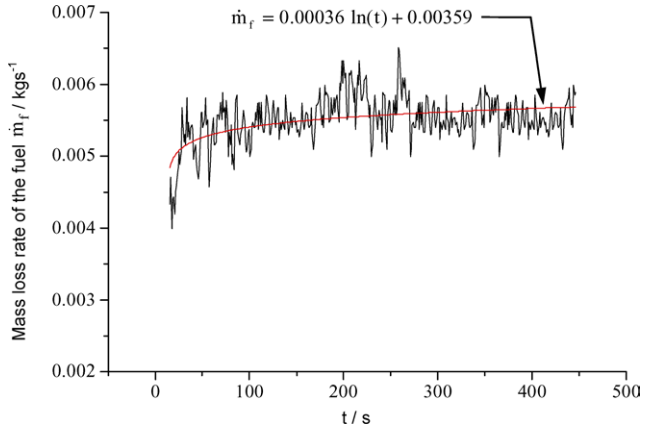


Fig. 3. Mass loss rate curve for test 1.

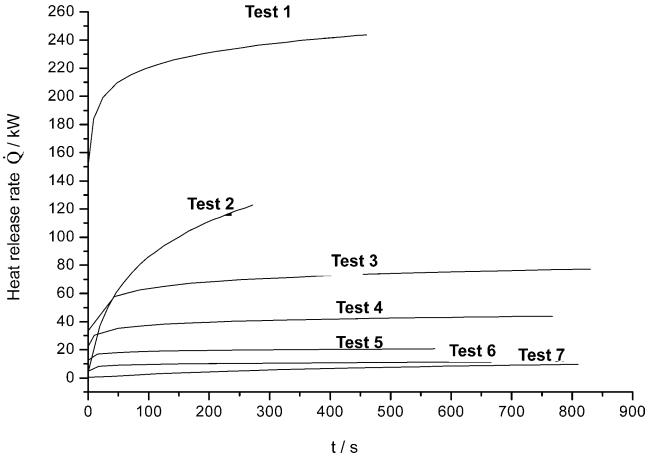


Fig. 4. Heat release rate curves for tests 1–7.

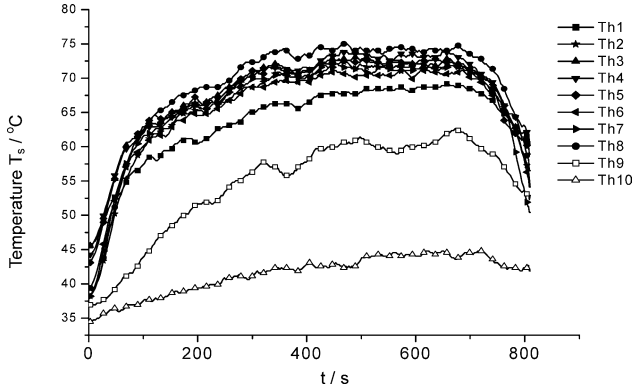


Fig. 5. Temperature distribution at T2 for test 4.

The width of the ventilation opening was kept at 1.6 m, the height was adjustable, which was 1 m in these tests. Mechanical ventilation of size 0.3 by 0.3 m was located on the top of the north wall, adjacent to the east wall. Hot smoke was extracted outside by the fan through the horizontal air ducts. The average flow velocity of the fan was measured to be 4.470 m·s$^{-1}$, thus the volumetric flow rate of mechanical exhaust was 0.4023 m$^3$·s$^{-1}$ (1448 m$^3$·h$^{-1}$).

Diesel of heat of combustion 42000 kJ·kg$^{-1}$ was used as the burning fuel in the experiments. Eight pool fire tests were carried out using square pans and circular pans of various sizes. The smoke layer temperature, the transient mass loss rate of fire source, and the steady elevation of smoke layer interface were measured. When smoke spilled out through the door opening, the outflow layer depth $H_s$ was also measured by a ruler.

## 4. Experimental results

Experimental conditions and results are shown in Table 1. The fire pools at an elevation $Z_b$ to the ground were put on an electronic balance at the center of the shop model. The burning time and depth of the fires are also shown.

### 4.1. Heat release rate

The heat release rate $\dot{Q}$ was calculated from the transient mass loss rate of the fuel $\dot{m}_f$, the combustion efficiency $\alpha$ and the heat of combustion $\Delta H_c$:

$$\dot{Q} = \alpha \dot{m}_f \Delta H_c \tag{21}$$

For pools of smaller size in this paper, sufficient air was supplied through the door for combustion, so $\alpha$ was taken as 1. A typical transient mass loss change rate curve for diesel pool fire in test 1 is shown in Fig. 3. A fitted function was used to give a smoother curve. HRR curves for all tests are shown in Fig. 4. All indicated that there was a growth stage before the HRR became steady.

### 4.2. Upper layer temperature

Typical temperature changes of the shop inside for test 4 measured by T2 are given in Fig. 5. As shown in the figure, the thermocouples labeled as 1 to 8 had relatively high temperatures, indicating that they were in the upper hot layer. Thermocouple 10 was beneath the elevation of smoke layer interface, thus the temperature measured was relatively lower. Thermocouple 9 was at about the edge of the interface of the hot smoke and cold air, so the temperature was a little lower than thermocouples 1 to 8 but higher than thermocouple 10. Operating the mechanical extraction system would give a thinner smoke layer at the opposite corner. The temperature of thermocouple 1 was lower than those at other thermocouples in the hot layer, which had approximately the same values. In a zone model, temperature in the hot smoke layer is assumed to be uniform. The average temperature of the whole upper layer was estimated from the thermocouples in the upper layer, which was estimated to have 5% uncertainty. The measurement error of temperature was estimated to be ±1 °C. A space average was performed for thermocouples 1 to 8 in test 4 to get the experimental average temperature of the upper layer.

Table 1
Experimental conditions and measured results

| Tests | Test 1 | Test 2 | Test 3 | Test 4 | Test 5 | Test 6 | Test 7 | Test 8 |
|---|---|---|---|---|---|---|---|---|
| Initial temperature inside the shop $T_0$ [°C] | 35 | 36.5 | 32 | 43 | 44 | 40 | 37 | 37 |
| Pool size [m$^2$] | $0.5 \times 0.5$ | $(0.5 \times 0.37)^2\pi$ | $0.33 \times 0.33$ | $0.28 \times 0.28$ | $0.23 \times 0.23$ | $0.18 \times 0.18$ | $0.13 \times 0.13$ | $0.33 \times 0.33$ |
| Burning time [s] | 500 | 376 | 850 | 840 | 650 | 741 | 841 | 500 |
| Pool depth [m] | 0.025 | 0.015 | 0.02 | 0.02 | 0.02 | 0.015 | 0.02 | 0.02 |
| Elevation height of fire [m] | 0.20 | 0.15 | 0.15 | 0.15 | 0.16 | 0.16 | 0.15 | 0 |
| Flame height [m] | $1.3 \pm 0.2$ | $1.0 \pm 0.2$ | $0.75 \pm 0.2$ | $0.55 \pm 0.15$ | $0.42 \pm 0.1$ | $0.35 \pm 0.1$ | $0.30 \pm 0.1$ | $0.80 \pm 0.2$ |
| Average heat release rate $\dot{Q}$ at steady burning stage [kW] | 238.22 | 116.4 | 74.70 | 42.04 | 20.13 | 10.84 | 8.41 | 74.70 |
| Average experimental upper layer temperature at stable stage $T_s$ [°C] | 186.71 | 107.05 | 81.47 | 71.34 | 58.20 | 47.77 | 42.54 | 82.29 |
| Smoke spill out? | Y | N | N | N | N | N | N | Y |
| Outflow depth [cm] | 3.5 to 7 | – | – | – | – | – | – | 2–10 |
| Steady height of smoke layer [m]: | | | | | | | | |
| Experiments | 0.93–0.96 | 1.10 | 1.28 | 1.47 | 1.65 | 1.85 | 2.10 | 0.9–0.98 |
| Heskestad | 0.885 | 1.179 | 1.375 | 1.586 | 1.859 | 2.174 | 2.303 | 1.235, 0.941* |
| Zukoski | 1.180 | 1.319 | 1.407 | 1.520 | 1.716 | 1.973 | 2.104 | 1.254, 0.978* |
| McCaffrey | 0.755 | 0.913 | 1.151 | 1.326 | 1.466 | 1.616 | 1.651 | 1.040, 0.805* |
| Thomas | 0.888 | 0.985 | 1.092 | 1.219 | 1.406 | 1.659 | 2.027 | 0.957, 0.807* |
| CFAST | 0.809 | 0.957 | 1.206 | 1.331 | 1.504 | 1.645 | 1.699 | 1.068 |

Note: $H_v = 1$, $W = 1.6$ m. The value marked with * in test 8 was the calculated height corrected by $C_i$.

### 4.3. Other variables during steady burning

The interface heights were measured at the steady burning stage and the results are listed in Table 1. The average temperature and $\dot{Q}$ derived from the time averaging over the steady burning period are shown in Table 1.

For diameter varied from 0.1 to 1 m, the burning would be in the transition regime. The burning rate depended on $D_f$, the fire characteristic length. From the eight diesel pool tests and a free burning test of a pool of diameter 0.7 m, a correlation equation was found:

$$\dot{Q} = 1952 D_f^3 \tag{22}$$

The pool perimeter corresponded to a certain $\dot{Q}$ for diesel pool fires will be calculated using the above equation for Thomas's correlation in this paper.

$H_k$ depends on too many factors and has to be estimated by experiments. For very thin solid walls, it can be supposed to be a process of stationary conduction in the wall. For no smoke spilling out at the steady burning stage, heat balance as in Eq. (4) gives:

$$\begin{aligned}\dot{Q}_{\mathrm{Loss},a} &= \dot{Q}_{c,a} - \dot{M}_{e,a} C_p (T_{s,a} - T_0) \\ &= H_k A_{s,a} (T_{s,a} - T_0)\end{aligned} \tag{23}$$

The subscript '$a$' refers to the average value during the steady burning stage. Substituting the experimental results listed in Table 1, $H_k$ can be fitted from tests 2–7, taken as $0.015\ \mathrm{kW \cdot m^{-2} \cdot K^{-1}}$.

The fraction of the total chemical energy of flame lost as radiation $\lambda r$ was found to be almost constant for a particular fuel. For smaller burners, this value is relatively independent of the burner size. The values of $\lambda_r$ were measured in two tests, tests 1 and 3. A radiometer was placed at $1.0 \pm 0.1$ m away from the center of the pool pan, pointing at the flame. A point source model was used to calculate the radiative heat loss fraction from the measured heat release rate and radiation heat flux data:

$$\lambda_r = \frac{4\pi L^2 \dot{q}_r}{\dot{Q}} \tag{24}$$

$\lambda_r$ in tests 1 and 3 were found to be 0.27 and 0.33, respectively. Therefore, taking $\lambda_r$ as approximately a constant of 0.3 is reasonable, giving 10% uncertainty. Accordingly, $\lambda_c$ was taken as 0.7 in this paper.

## 5. Numerical experiments

Eqs. (1) and (2) were used for predicting the mechanical exhaust part of the model developed for fires in a typical shop. In this model, there are four choices of plume models.

The two equations are used to predict the interface height and temperature:

$$-\rho_s A_c \frac{\mathrm{d}Z}{\mathrm{d}t} = \begin{cases} \dot{M}_p & (H_{em} + H_e/2 < Z < H_c) \\ \dot{M}_p - \big[(H_{em} + H_e/2 - Z)/H_e\big]\dot{M}_e & (H_{em} - H_e/2 < Z < H_{em} + H_e/2) \\ \dot{M}_p - \dot{M}_e & (H_v < Z < H_{em} - H_e/2) \\ \dot{M}_p - \dot{M}_e - \dot{M}_s & (Z_0 + Z_b < Z < H_v) \end{cases} \tag{25}$$

$$\begin{aligned}&\rho_s A_c (H_c - Z) C_p \frac{\mathrm{d}T_s}{\mathrm{d}t} \\ &\quad = \dot{Q}_c - \dot{M}_p C_p (T_s - T_0) \\ &\qquad - H_k \big[2A_c + P_e (H_c - Z)\big](T_s - T_0)\end{aligned} \tag{26}$$

In some cases as shown later, $\dot{M}_i$ should also be included, so $\dot{M}_p$ was multiplied by a constant $C_i$ in the model for describing mass exchanges at the smoke layer interface.

The iteration was performed by the following steps:

$$Z_{n+1} = Z_n - \left[\left(\sum \dot{M}_{j,n}\right)\Delta t\right]/(A_c\rho_{s,n}) \tag{27}$$

$$T_{s,n+1} = T_{s,n} + \left\{\left[\lambda_c \dot{Q}_n - \dot{M}_{p,n}C_p(T_{s,n} - T_0) - H_k A_{s,n}(T_{s,n} - T_0)\right]\Delta t\right\}/(m_n C_p) \tag{28}$$

$$\rho_{s,n+1} = 1.22\left(\frac{290}{T_{s,n+1} + 273}\right) \tag{29}$$

$$m_{n+1} = \rho_{s,n+1}A(H_c - Z_{n+1}) \tag{30}$$

Among $\dot{M}_{j,n}$, the mechanical exhaust rate $\dot{M}_e$ was calculated by the following equation:

$$\dot{M}_{e,n} = \rho_{s,n}V_e A_e = 1.22\left(\frac{290}{T_{s,n} + 273}\right)V_e A_e \tag{31}$$

The entrainment rate of plume $\dot{M}_p$ at a height $Z$ was estimated from the heat release rate $\dot{Q}$ by the four plume models:

$$\dot{M}_{p,n} = \phi\left(Z_n, \dot{Q}_n\right) \tag{32}$$

The heat release rate $\dot{Q}$ was fitted by a logarithm function from experimental data on mass loss rate:

$$\dot{Q}_n = \left[a\ln(n\Delta t + t_i) + b\right]42000 \tag{33}$$

Initial conditions were:

$$Z_0 = H_c, \qquad T_{s,0} = T_0$$

$$\dot{Q}_0 = \left[a\ln(t_i) + b\right]42000 \tag{34}$$

For the bottom of the fire at a height $Z_b$ above the ground, the actual height $Z'$ with air entrainment to the plume is given by:

$$Z' = Z - Z_b - Z_0 \tag{35}$$

If smoke spread out from the shop through the door, $Z$ would be approximately equal to $H_n$ in the calculation process. This was well-demonstrated in the tests with a stratified smoke layer.

$$H_s = H_v - Z = H_v - \left(Z' + Z_b + Z_0\right) \tag{36}$$

Based on the above assumptions, the smoke layer temperatures and interface heights were predicted as shown in Figs. 6–13 together with the experimental results. Those results predicted by CFAST v5.01 are shown as well.

The following can be observed from these figures and Table 1:

*I.* A smoke layer was found in all tests as confirmed by temperature measurement and visual observations. The developed fire mode with mechanical exhaust gives good predictions and is suitable for simulating retail shop fires.

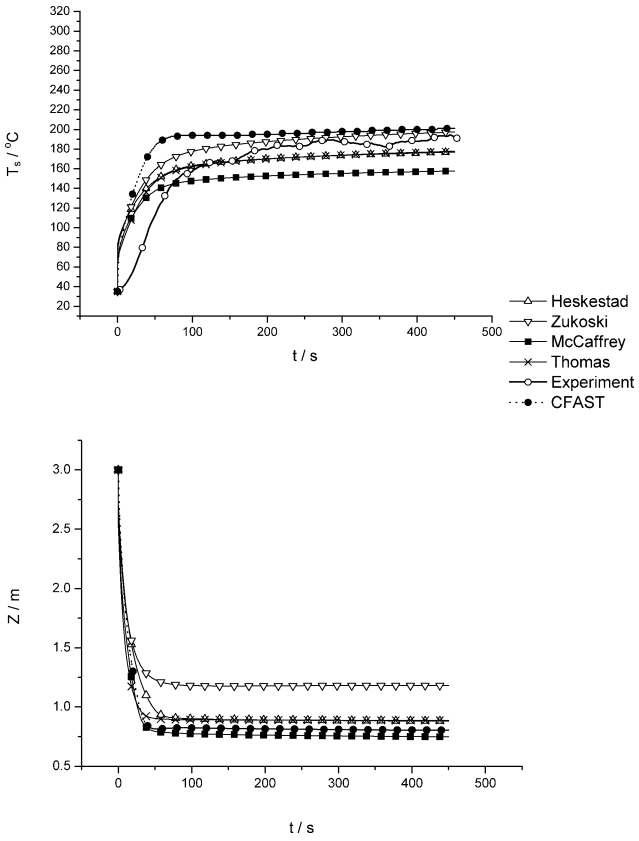


Fig. 6. Comparison of results predicted by the four plume models and CFAST with experiment for test 1.

*II.* Different smoke layer temperature and interface height were predicted by the four plume models. For smoke not spilling out in the calculation process, the temperature rise was related to the plume model selected in the initial growth stage. However, the values of temperature rise were similar during the steady burning process for all four models as shown in Figs. 8–12. When spilling was predicted by a plume correlation, the temperature rise curve would be different from the others. For example in Fig. 7, lower temperature rise was predicted from the McCaffrey's and Thomas's correlation because smoke spilled out in the calculation process. The development of the smoke layer interface height was found to be related with the plume correlation for all tests. Possible explanations are:

At the steady burning stage, the smoke layer interface height might be quite stable. When there was no smoke spilling out, mass conservation given by Eq. (1) would be:

$$\dot{M}_e = \dot{M}_p \tag{37}$$

Energy equation given by Eq. (2) for $\frac{dT_s}{dt}$ tends to zero can be written as:

$$\dot{Q}_c = \dot{M}_e C_p(T_s - T_0) + H_k A_s(T_s - T_0) \tag{38}$$

Different smoke layer interface heights would be predicted by Eq. (37) for the four plume models with the same heat release rate $\dot{Q}$. The temperature curves increased in a similar way but depended on $\dot{Q}$ and the mechanical exhaust rate.

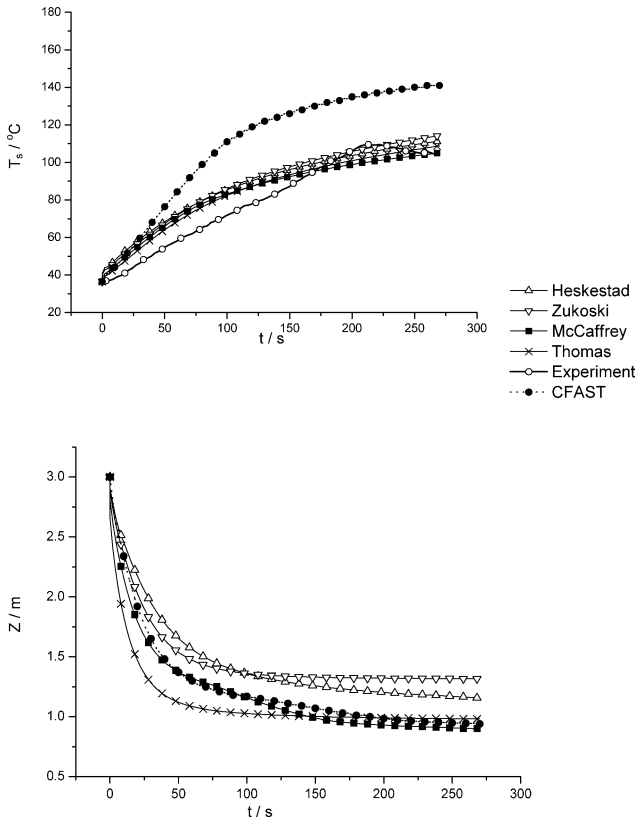


Fig. 7. Comparison of results predicted by the four plume models and CFAST with experiment for test 2.

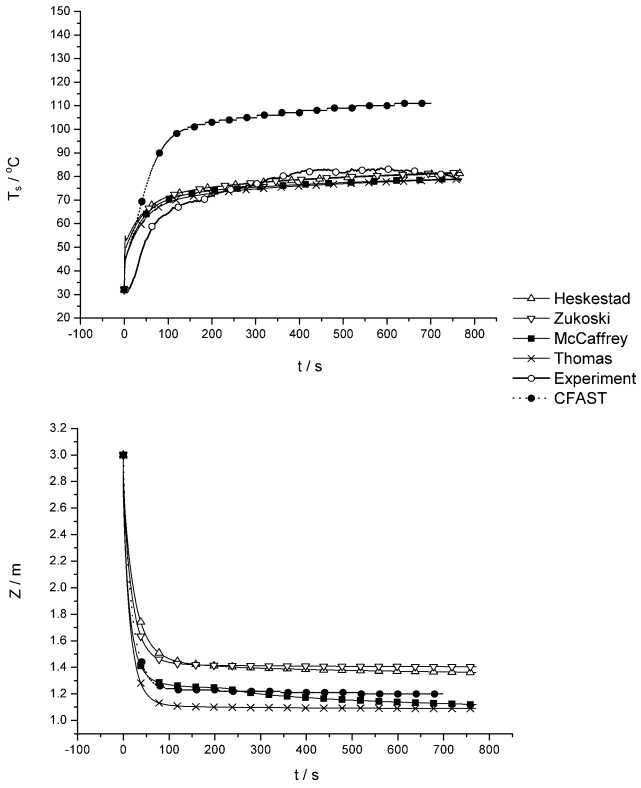


Fig. 8. Comparison of results predicted by the four plume models and CFAST with experiment for test 3.

If smoke spilled out through the door opening at the steady burning stage, then:

$$\dot{M}_p = \dot{M}_e + \dot{M}_s$$
$$\dot{Q}_c = \dot{M}_p C_p (T_s - T_0) + H_k A_s (T_s - T_0) \quad (39)$$

Therefore, both the stable smoke layer interface height and smoke temperature are related to the plume model selected.

*III.* The upper layer temperatures predicted by CFAST were higher than the experimental results, which in part could be caused by the method of calculation of heat losses through the compartment boundaries. Heat losses through the compartment were predicted to be less than the actual heat losses. This observation is consistent with other published comparisons of test data with CFAST predictions [12]. A possible reason is on solving the transient thermal conduction numerically with coarse grids. The results predicted by this developed mechanical exhaust model agreed better with experiments. The smoke layer interface heights simulated by CFAST were similar to those predicted by this model while using McCaffrey's plume model. That is because this plume model was used in CFAST.

*IV.* Different plume correlations would give different steady smoke layer interface heights and similar uncertainties in the mechanical exhaust design. It is difficult to say which model is better. In fact, the predicted results can be better or worse than the experiment data for different fires. For example, Zukoski's correlation predicted smoke would not spill out in test 1. The other three plume correlations predicted that smoke would spill out. The results of Heskestad's and Thomas's correlations agreed better with the experiments. But Zukoski's correlation gave better predictions on the measured heights than the other models for smaller heat release rates. It appears that the four plume correlations have their own validity limit for different heat release rates.

## 6. Analysis

Smoke layers were observed to be stratified in all the tests. From the experimental results as summarized in Table 1, the smoke layer was kept at a certain height with mechanical exhaust, though there was some smoke spilling out in tests 1 and 8. It was obvious that the smoke produced by the pool fires was controlled by mechanical exhaust efficiently in retail shop fires. Comparing the experimental data with the calculated results through different correlations and CFAST, it can be concluded that the two-zone model, as illustrated in Fig. 1, is well applicable to the prediction of the steady height and the upper layer temperature with mechanical exhaust. The effect of fire bottom elevation $Z_b$ should be noted, the pool size of tests 3 and 8 were the same, but the pool in test 8 was placed on the ground, so more air was entrained into the flame region. And the mass flow rate into

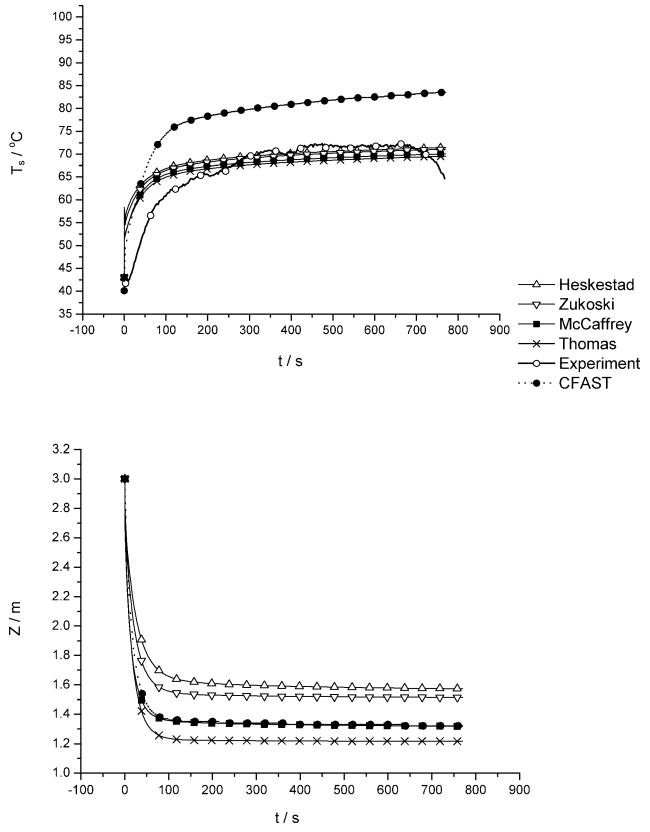


Fig. 9. Comparison of results predicted by the four plume models and CFAST with experiment for test 4.

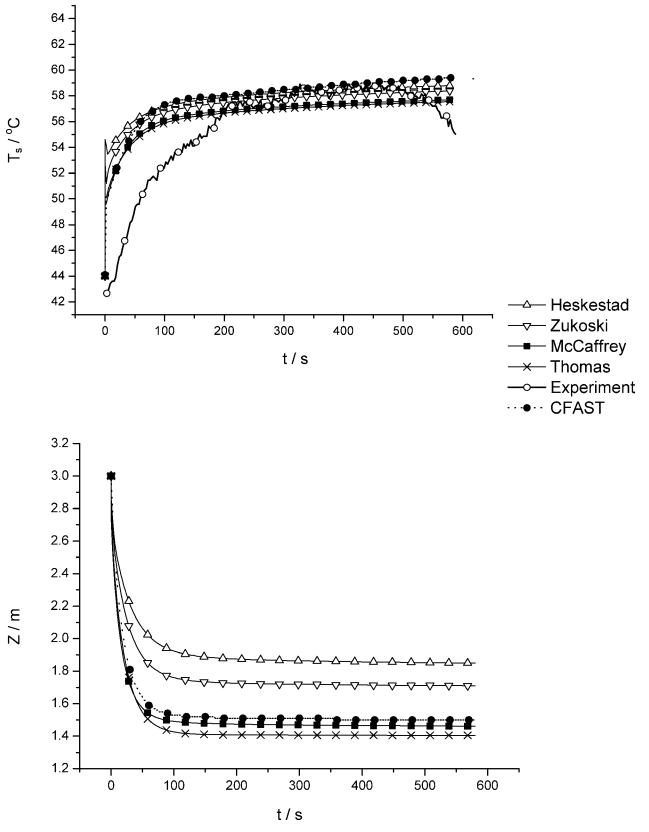


Fig. 10. Comparison of results predicted by the four plume models and CFAST with experiment for test 5.

the hot layer would also increase as the distance increased. Besides, the smoke layer interface for test 8 was observed to fluctuate strongly during the experiment, which resulted in the increase of the mass exchange $M_i$ at the interface between the smoke layer and the lower cold air layer, so the mass flow into the hot layer increased to cause the spill.

For the predicted results of test 8 as shown in Fig. 13, except for Thomas's correlation, there was no outflow in the other three correlations' calculation results, which is just because $M_i$ was neglected. In zone model, only the mass and energy exchange between the plume and the hot layer are taken into account, so when the fluctuation is great, the deviation of calculation will be much enlarged. This fluctuation was also observed in test 7, the smoke layer interface elevation was so near to the mechanical exhaust opening that the fan's extraction had made a great impact on the smoke layer interface. So, the influence of mechanical exhaust and door opening on $\dot{M}_i$ and $\dot{M}_p$ in zone model should be taken into account. It is proposed that when the disturbance and fluctuation is relatively strong, the mass flow rate into the hot layer may be corrected by the plume entrainment rate multiplied by a constant coefficient $C_i$. In comparing the experimental results with the predicted results, it is suggested that $C_i$ might be taken from 1.00 to 1.60 under the experimental conditions of this paper. That was deduced from the mass conservation equations. Smoke layer height of test 8 calculated by taking $C_i$ to be 1.60 are shown in Fig. 14 and Table 1. The results agreed better with the experiments.

For fire safety design, the mechanical exhaust rate should be calculated by considering more practical factors relevant to the heat release rate of fire $\dot{Q}$, the fire width $D_f$, the elevation of fire bottom $Z_b$, the height expected to be kept $Z$, the fluctuation of smoke layer interface and the plume correlation. For relatively small fires, the critical exhaust rate to keep no outflow through the door opening can be calculated as:

$$\dot{M}_e = 0.076\dot{Q}^{1/3}\left\{Z - \left[0.01\left(\dot{Q}/D_f\right)^{2/3} - 0.80D_f\right] - Z_b\right\}^{5/3}C_i \tag{40}$$

From the predicted results of the tests, different plume models would give different results. As the plume mass fluxes are different, expressions should be compared and analyzed first. To compare the plume models, the four plume correlations were approximately written in a uniform form for near field and the plume region far away to a height where $Z_0$ can be neglected, by the correlation Eq. (22) between the heat release rate $\dot{Q}$ and pool diameter $D_f$ for diesel pool fires of diameter 0.13–0.7 m,

$$\dot{M}_p = C D_f^{\gamma} Z^{\eta} \tag{41}$$

where $C$, $\gamma$, $\eta$ are approximately equal to the values listed in Table 2.

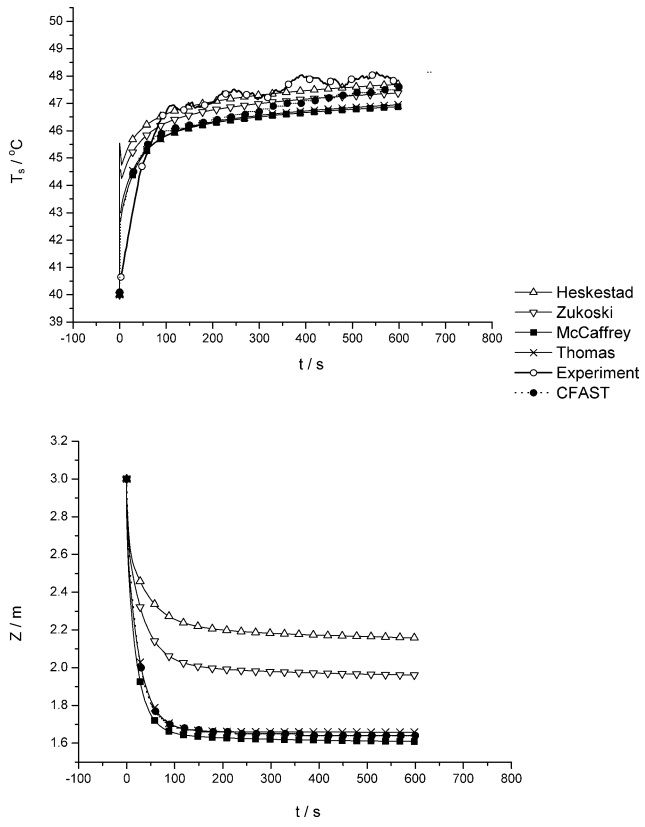


Fig. 11. Comparison of results predicted by the four plume models and CFAST with experiment for test 6.

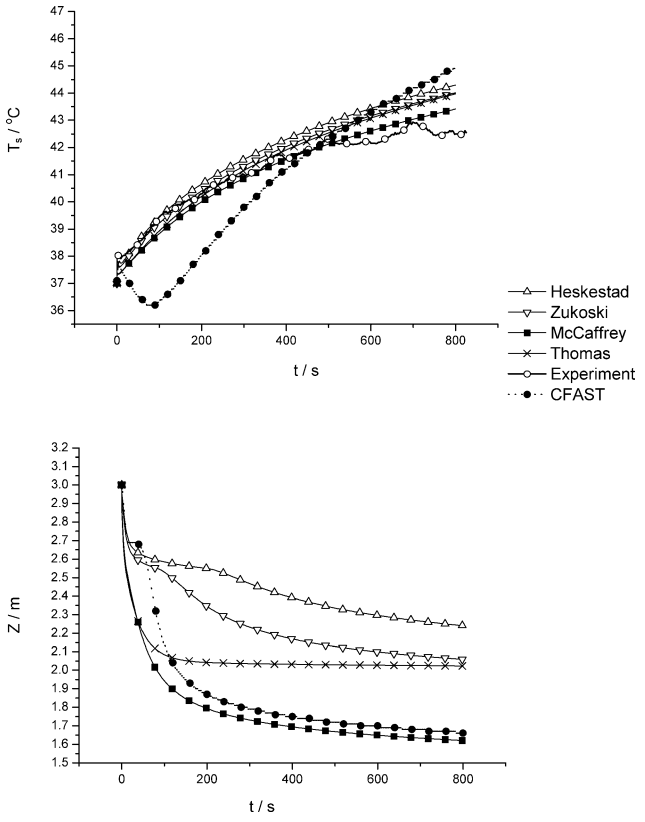


Fig. 12. Comparison of results predicted by the four plume models and CFAST with experiment for test 7.

The plume mass flux given by the models are significantly different, and increase with different coefficient and exponents of $D_f$ and $Z$.

The plume mass flux at a height $Z$ predicted by the four plume models are shown in Fig. 15, Z changed from floor to typical ceiling height in retail shop fires. A bigger fire and larger $Z$ were tested as in Fig. 16 to observe the far field effects. The steady heights predicted by mechanical exhaust model with the four plume correlations and CFAST at the stable stage are listed in Table 1, which are shown in Fig. 17 for tests 1–7. Fig. 18 compared the plume mass flow rate at the experimental steady interface height given by experiments and the four plume correlations for tests 2–7.

The mass flux predicted by Zukoski's correlation is 20% higher than that of Heskestad in the far field of the plume as shown in Figs. 15 and 16. However, the predicted results are lower in the near field including the flame region and the near plume region over the top of the flame. Zukoski's correlation for the far field plume was derived from the classical weak point source theory based on a similarity between excess temperature $\Delta T$ and upward velocity $w$. The Boussinesq approximation was applied ($\rho_0 = \rho$) in some equations. This might not be appropriate for strong plumes, like plumes near the flame and near the burner, or plumes from large fires where the difference of density between the plume and ambient air is much larger. The entrainment coefficient of the correlation for the far plume was derived from experimental

Table 2
Approximate constants in uniform form for the four plume models

| Model | Region | $C$ | $\gamma$ | $\eta$ |
|---|---|---|---|---|
| Zukoski | Near field | 0.62 | 1 | 0.750 |
| | Far field | 0.949 | 1 | 1.667 |
| Heskestad | Near field | 1.897 | 1.273 | 1 |
| | Far field | 0.788 | 1 | 1.667 |
| | Continuous region | 3.863 | 2.321 | 0.566 |
| McCaffrey | Intermittent region | 3.2287 | 1.909 | 0.909 |
| | Far filed | 0.776 | 0.726 | 1.895 |
| Thomas* | Entire region | 1.348 | 1 | 1.5 |

* Eq. (16).

data of fires from 10 to 200 kW. It is more suitable for modeling small fires at the far field of the smoke plume, which was shown by the experiments as in Fig. 17. The heights calculated by Zukoski's correlation were in good agreement with the experiment when the heat release rate of the fire was less than 75 kW with diameters 0.13–0.33 m, in which the smoke layer was kept at the far field for $(Z - Z_b)/D_f > 3.5$. The mass fluxes of plume were also similar with the experiments as shown in Fig. 18. But when the heat release rate of the fire increased to over 75 kW, the deviation of smoke layer height and mass flux between the experiments and predictions of Zukoski's correlation became larger. It seemed to be not suitable for large fires and the steady smoke layer

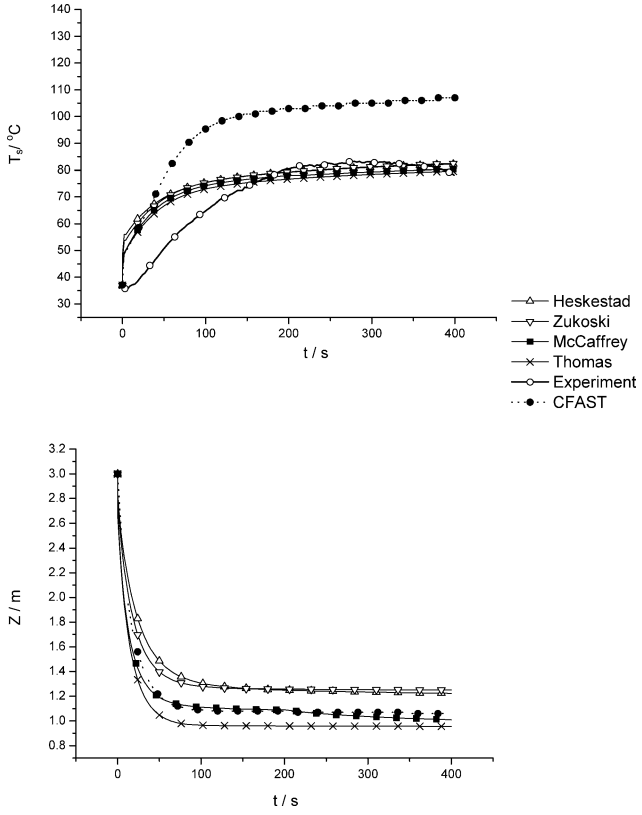


Fig. 13. Comparison of results predicted by the four plume models and CFAST with experiment for test 8.

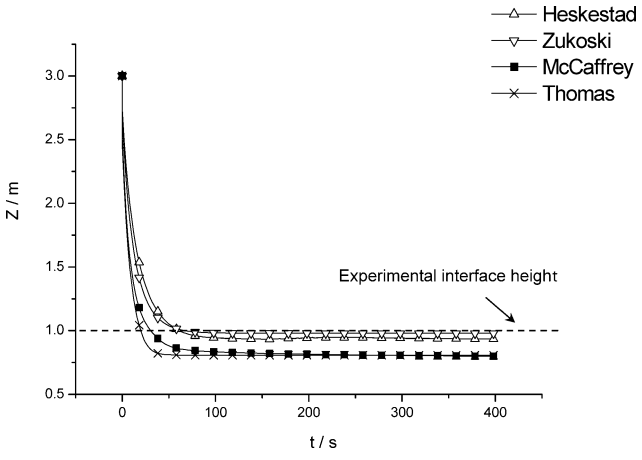


Fig. 14. Results predicted by this model corrected by $C_i = 1.6$ for test 8.

height descending to the near field and flame region. In the near field, Zukoski's correlation was obtained by experimental data from 60 kW natural gas of diameter 19 cm and 21, 42, 50 kW of diameter 50 cm. The small power of the fires are not expected to give better results for larger fires.

Heskestad's correlation was obtained based on the similarity between upward velocity $w$ and density deficit $\Delta\rho$, large density differences could be taken into account. The equations discussed by Heskestad were said to describe strong plumes. It was shown in Figs. 17 and 18 that the smoke layer height predicted by Heskestad's correlation was

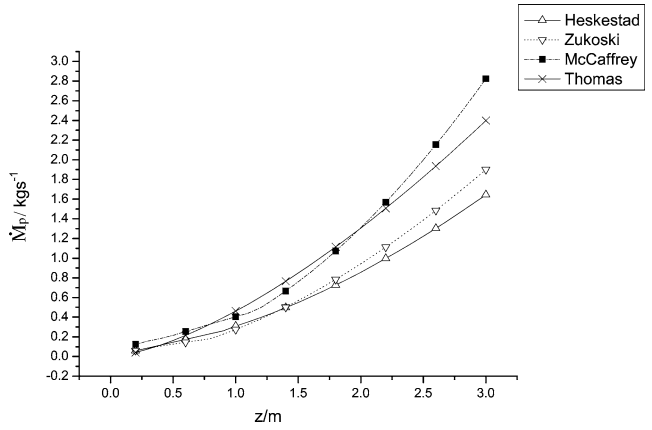


Fig. 15. Plume mass flux at a height $Z$ predicted by the four plume models, $\dot{Q} = 74.70$ kW (test 3), $Z_{fl} = 0.97$ m.

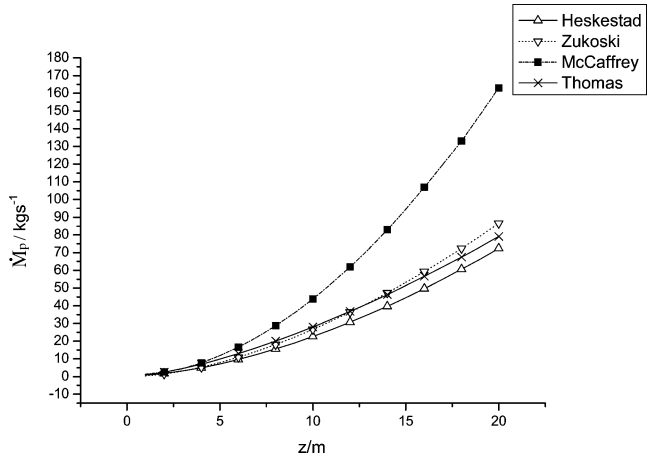


Fig. 16. Plume mass flux at a height $Z$ predicted by the four plume models, $\dot{Q} = 500$ kW, $Z_{fl} = 2.15$ m.

slightly higher than the experimental results and the mass flux was underpredicted in tests 4–7, which had a relative small heat release rate less than 75 kW and the interface height was at the far field. However, better agreement could be obtained than Zukoski's correlation for fires of 75–240 kW with diameters 0.33–0.5 m and steady smoke layer interface height stayed in the near field $(Z - Z_b)/D_f < 3$. Therefore, Heskestad's correlation is more applicable to describe relatively large fires and the details of near field plume. It might be in part due to the fact that the correlation was based on large-scale experiments involving relatively high heat release rate and realistic fuel package.

When comparing the mass flux predicted by McCaffrey's correlation with others, it could be found that the mass flux predicted by McCaffrey's correlation is about 10% higher than Heskestad's and Zukoski's in the equations field. Deviation increased with $Z$ up to the far field, almost doubling the former two equations as shown in Fig. 16. By comparison with the experiments, the interface height and mass flux predicted by McCaffrey's correlation were found to be greatly satisfactory with the measured results in test 3 (see Figs. 17

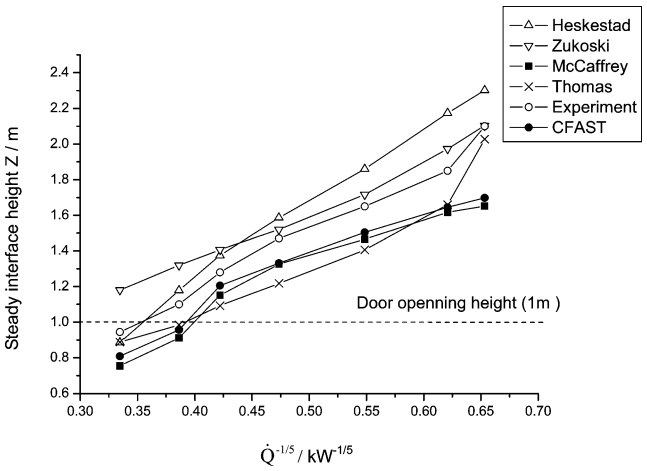


Fig. 17. Comparison of the smoke layer height by experiments and calculations with different plume correlations for tests 1–7.

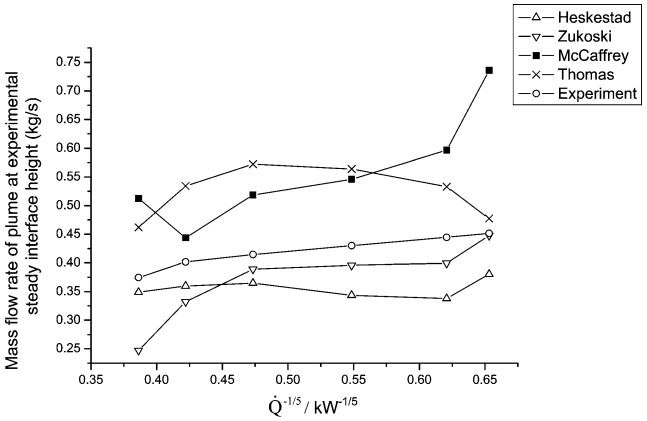


Fig. 18. Comparison of the plume mass flow rate at the experimental steady interface height by experiments and the four plume correlations for tests 2–7.

and 18), the interface of which $Z - Z_b$ was about $1.15Z_{fl}$, stayed in the intermittent flame region. However, with the heat release rate increased or the interface moving away to the far field, the interface heights were to a certain extent lower, the mass fluxes were all found to be overpredicted except in test 3, as shown in Fig. 18. The possible reasons are that for large fires, the structures of flames may be different from the small flames for the turbulence. McCaffrey's correlation was just validated by relatively small methane fires of heat release rates 14.4, 21.7, 33.0, 44.9 and 57.5 kW by measuring the average temperature and upward velocity distribution. Besides, the behavior of diesel fire may not be common with the methane fires for the fuels have different luminosity, radiation losses vary considerably, and the flame temperature varies from fuel to fuel. These effects should be noted and may cause deviation for different fuels. The smoke layer interface heights simulated by CFAST were similar to those predicted by this model while using McCaffrey's plume model.

As shown in Figs. 15 and 16, the mass flux predicted by Thomas's correlation were higher than those by Heskestad's and Zukoski's correlation for diesel pool fires. But the results were lower than those by McCaffrey's model, except for a section from the top part of the intermittent region to the near filed of the smoke plume. Note that there are three regimes in McCaffrey's expression. And the value by Thomas's correlation would be less than those by Zukoski and Heskestad at a large height $Z$ in the far field of the smoke plume region, for its mass flux increases with a smaller exponent of $Z$ than the former two. By comparison with the experiments, the predictions by Thomas's correlation were similar with the measured results for fires of tests 1 and 2 with a relatively large area of diameter 0.37–0.5 m, the interfaces of which were both kept in the near field. For tests 3–7, the results were unsatisfactory, its prediction of mass entrainment was a little higher to give a lower interface height. Thomas's correlation was just validated by fires of a relatively larger area ($D_f > Z_{fl}$) and seemed simple to describe the plume characteristics of small area fires. However, since it is simple for calculation and stays on the safe side of the prediction, it is still used extensively in engineering applications.

## 7. Conclusion

The two-layer mechanical exhaust model in the present model, which is developed for retail shop fires, is observed to be in good agreement with the experiments on mechanical extraction. The temperature predicted by CFAST would be a little higher than the experiments, but the key height would be approximately the same as the ones predicted by McCaffrey's correlation in the present model. At steady burning stage, mechanical exhaust may keep the steady smoke layer interface at a certain height well, which can be predicted by the mechanical exhaust rate $\dot{M}_e$ and heat release rate $\dot{Q}$ and other practical factors.

When the fluctuation is great, the influence of mechanical exhaust and door opening on $\dot{M}_i$ and $\dot{M}_p$ in zone models should be taken into account. In zone models, only the mass and energy exchange between the plume and the hot layer are taken into account, so the prediction of the total mass flow rate into the upper layer should be corrected by a coefficient $C_i$ with the increase of $\dot{M}_i$.

To predict the fire environment in retail shops with mechanical exhaust, a suitable choice of plume model depends on the parameters of the actual cases, such as the heat release rate $\dot{Q}$, fire diameter $D_f$, the properties of fuel packages $\Delta H_c$, $\lambda_c$, and also the estimated interface height of the smoke layer. When smoke was kept above the opening height, the temperature rise of the steady stage was shown to be less related to the plume models, and more related to the property of the wall material, the heat release rate and the mechanical exhaust rate. But if the smoke spilled out the opening, the temperature rise would be related to the choice of the plume models. In predicting the steady smoke layer height at a certain mechanical extraction rate, there are deviations between the experiments and calculations with differ-

ent plume models. It is not easy to say which plume model is better, however, confirming the applicable limits may be more realistic. Under the conditions described in this paper, Zukoski's correlation can be applied to study small fires of heat release rate less than 75 kW with diameters 0.13–0.33 m, and is more suitable for describing the far field of plume for $(Z - Z_b)/D_f > 3.5$. For large fires of 75–240 kW with diameters 0.33–0.5 m, or steady smoke layer interface height stayed in the near field $(Z - Z_b)/D_f < 3$, such as flame plunging into the smoke layer, it appears that Heskestad's correlation works well. If the smoke layer is kept at the intermittent flame region, see that $Z - Z_b$ is about $1.15Z_{fl}$ for fires of 75 kW, McCaffrey's correlation is recommended. However, Thomas's correlation might not be a good choice for small area fires, such as for fires of 0.13–0.33 m, but better predictions were expected for the near field of the fires of a relatively larger area, say fires of diameters 0.37–0.5 m.

## References

[1] E.E. Zukoski, T. Kubota, B. Cetegen, Entrainment in fire plumes, Fire Safety J. 3 (3) (1980) 107–121.
[2] G. Heskestad, Engineering relations for fire plumes, Fire Safety J. 7 (1) (1984) 25–32.
[3] B.J. McCaffrey, Momentum implications for buoyant diffusion flames, Combust. Flame 52 (2) (1983) 149–167.
[4] P.H. Thomas, P.L. Hinkley, C.R. Theobald, D.l. Simms, Investigations into the flow of hot gases in roof venting, Fire Research Technical Paper 7, London: HMSO, 1963.
[5] R.D. Peacock, G.P. Forney, P. Reneke, R. Portier, W.W. Jones, CFAST, the Consolidated Model of Fire Growth and Smoke Transport, NIST Technical Note, vol. 1299, National Institute of Standards and Technology, 1993.
[6] NFPA 92B, Guide for Smoke Management Systems in Malls, Atria, and Large Areas, National Fire Protection Association, Quincy, MA, 1991.
[7] J.G. Quintiere, Fundamentals of enclosure fire "zone" models, J. Fire Protection Engrg. 1 (3) (1989) 99–119.
[8] C.M. Fleischmann, P.J. Pagni, R.B. Williamson, Salt water modeling of fire compartment gravity currents, Fire Technol. 30 (1993).
[9] B.R. Morton, G.I. Taylor, J.S. Turner, Turbulent gravitational convection from maintained and instantaneous sources, Proc. Roy. Soc. A 234 (1956) 1–23.
[10] B.M. Cetegen, E.E. Zukoski, T. Kubota, Entrainments in the near and far fields of fire plumes, Combust. Sci. Technol. 39 (1984) 305.
[11] H.W. Emmons, "Vent Flows" SFPE Handbook of Fire Protection Engineering, second ed., National Fire Protection Association, Quincy, MA, 1995.
[12] P.A. Reneke, M.J. Peatross, W.W. Jones, C.L. Beyler, R. Richards, A comparison of CFAST predictions to USCG real-scale fire tests, J. Fire Protection Engrg. 11 (1) (2001) 43–68.